Helal, Y., Garcia, R., Pilakoutas, K., Guadagnini, M. & Hajirasouliha, I. (2016), "Strengthening of short splices in RC beams using Post-Tensioned Metal Straps", Materials and Structures, 49:133. https://doi.org/10.1617/s11527-014-0481-6

Strengthening of short splices in RC beams using Post-Tensioned Metal Straps

Yasser Helal, Reyes Garcia*, Kypros Pilakoutas, Maurizio Guadagnini, Iman Hajirasouliha

Dept. of Civil and Structural Engineering, The University of Sheffield, Sir Frederick Mappin Building, Mappin Street, Sheffield, S1 3JD, UK.

Tel.: +44 (0) 114 222 5071

Fax: +44 (0) 114 222 5700

Email (corresponding author*): r.garcia@sheffield.ac.uk

Abstract

This paper investigates the effectiveness of a novel and cost-effective strengthening technique using Post-Tensioned Metal Straps (PTMS) at enhancing the bond behaviour of short lap spliced steel bars in reinforced concrete (RC) beams. Twelve RC beams with a short lap splice length of $10d_b$ (d_b=bar diameter) at the midspan zone were tested in flexure to examine the bond splitting failure. The effect of confinement (no confinement, internal steel stirrups or external PTMS), bar diameter and concrete cover were examined. The results show that, whilst unconfined control beams failed prematurely due to cover splitting, the use of PTMS confinement enhanced the bond strength of the spliced bars by up to 58% and resulted in a less brittle behaviour. Based on the test results, a new analytical model is proposed to predict the additional bond strength provided by PTMS confinement. The model should prove useful in the strengthening design of substandard lap spliced RC elements.

Keywords: Lap splice; Seismic strengthening; RC beams; Bar slip; Confinement; Post-Tensioned Metal Straps

1. Introduction

Much of the existing RC building stock in many countries was designed primarily to sustain gravity loads with little or no seismic detailing, resulting in high vulnerability during earthquakes. Many catastrophic failures in such buildings during recent major earthquakes (e.g. Kashmir, 2005; China, 2008; Indonesia,

2009; Haiti, 2010; Turkey, 2011; Italy 2009 and 2012) were attributed to failure of substandard short lap spliced reinforcement, which was usually provided at locations of large demand such as the column-footing interface or above beam-column joints (see Fig. 1). These lap splices have typical lengths of $l_b \approx 20\text{-}24d_b$ (d_b=bar diameter), which are shorter than the splice lengths specified by bond provisions of modern design guidelines (ACI Committee 408 2012; fib 2013) (usually requiring $l_b > 40\text{-}60d_b$), and thus insufficient to mobilise the full capacity of the spliced bars. The strengthening of substandard lap spliced members can reduce the seismic vulnerability of existing substandard RC buildings, thus reducing social and economic risks.

Fig. 1 Lap splice failure at the bottom of a RC column (2005 Kashmir earthquake; credit: S. Ahmad)

Several techniques were utilised in the past to strengthen RC elements with short lap splices, such as confining spirals (Tepfers 1988) RC jacketing with internal or external steel stirrups (e.g. Coffman et al. 1993; Lynn et al. 1996; Melek et al. 2003), steel jacketing (e.g. Chai et al. 1991; Aboutaha et al. 1996; ElGawady et al. 2010), fibre reinforced concrete, concrete or shotcrete jacketing (e.g. Bousias et al. 2007; Karayannis et al. 2008; Beschi et al. 2011), and more recently external confinement using Fibre Reinforced Polymers (FRP) (e.g. Priestley and Seible 1995; Sause et al. 2004; Breña and Schlick 2007; Harajli 2008; Bournas and Triantafillou 2011). All the above strengthening techniques were proven effective at enhancing the bond strength of substandard splices. In comparison to unconfined splices, average enhancements in bond strength were reported to be 50-65% for splices confined with steel stirrups with two or three links, and 30-70% for splices confined with one or two layers of FRP. However, steel and

concrete/shotcrete jacketing interventions are usually highly invasive, labour intensive, time-consuming and can disrupt the functionality of the building. Concrete/shotcrete jacketing also increases the building mass, which places higher seismic demands on the building. On the other hand, the initial cost of FRP may discourage their use as strengthening solution in low and medium income developing countries. As a consequence, it is necessary to develop less disruptive and more cost-effective strengthening solutions for RC components with substandard spliced bars.

Early research at the University of Sheffield (Frangou et al. 1995) led to the development of a novel Post-Tensioning Metal Strapping (PTMS) technique for strengthening RC beams and columns. The technique involves the post-tensioning of ductile metal straps around RC elements using pneumatic steel strapping tools as those used in the packaging industry (see Video 1 in Supplementary Material). After post-tensioning, the straps are fastened mechanically using push-type seals and jaws to maintain the tensioning force. This provides active confinement to members, thus increasing their ductility and capacity even before loading. In comparison to other strengthening techniques, PTMS strengthening has advantages such as ease and speed of application, low material cost, ease of removing/replacing damaged straps, and flexibility to strengthen different types of structural elements. The PTMS strengthening can be applied very easily around RC columns (e.g. Moghaddam et al. 2010), whereas anchoring plates are necessary to secure the PTMS on beams and beam-column joints where the metal straps cannot be installed due to an existing slab. Such anchoring solution was proven effective at securing the PTMS strengthening on a substandard full-scale RC building tested recently by the authors (Garcia et al. 2014a). Overall, the use of PTMS for strengthening substandard buildings is expected to provide fast and more cost-effective solutions in comparison to the other traditional strengthening methods, especially in developing countries where the material cost accounts for the main expense of strengthening.

Research by Moghaddam et al. (2010) examined the effectiveness of the PTMS technique at enhancing the compressive strength of 72 small-scale column specimens confined with PTMS using different confinement ratios (i.e. different

strap spacing and number of strap layers). The results indicated that the PTMS technique was very effective at enhancing the strength and ductility of the concrete columns. The use of high confinement ratios (e.g. two layers of metal straps and no strap spacing) generally led to the largest enhancements. Samadi et al. (2012) performed cyclic tests on 2/3-scale RC circular columns with substandard lap splices confined with PTMS. To replicate typical substandard detailing of developing countries, the longitudinal bars were lap spliced at the column base for a length of $20d_b$ (d_b=bar diameter), which was insufficient to develop their yield capacity. Samadi et al. (2012) examined the effect of using different levels of post-tensioning force and layouts of straps. Whilst the control specimens failed prematurely due to bond splitting, the use of PTMS confinement enhanced the capacity of the columns by up to 17% and led to a more ductile behaviour. However, Samadi et al. only tested columns with circular cross section and, therefore, it is necessary to assess the effectiveness of the PTMS technique at enhancing bond strength of splices in rectangular RC components where the confinement is only effective at the corners. Moreover, it is also necessary to investigate the effect of active PTMS confinement on the bond-slip behaviour of lap spliced bars failing by cover splitting. In this case, the active confining pressure provided by the straps is expected to increase bond strength and delay cover splitting (Gambarova and Rosati 1997; fib 2000).

The bond behaviour of lap splices confined with internal steel stirrups has been examined using flexural tests on beams with short lap splices at the midspan (Orangun et al. 1977; Sozen and Moehle 1990; Zuo and Darwin 2000; Harajli 2006), as well as staggered splices (Cairns 2014; Metelli et al. 2014). Results from the former tests were used to develop the bond design equations included in modern design guidelines (ACI Committee 408 2012; fib 2013). This paper examines the behaviour of short lap splices in RC beams confined with PTMS. Twelve simply supported beams were designed to fail by bond-splitting at the midspan, where the main bottom reinforcement was spliced. PTMS confinement was provided at this zone to study the effect on the bond-slip behaviour of the splices and the overall behaviour of the beams. Based on the results of this study, a new analytical model is proposed to predict the additional bond strength provided by PTMS confinement. The work presented is part of an ongoing

comprehensive research programme focusing on seismic risk assessment (Ahmed 2011; Mulyani 2013) and strengthening of typical substandard RC structures using PTMS (Helal 2012; Garcia et al. 2014a) and FRP composites (Garcia et al. 2010; Garcia et al. 2014b; Garcia et al. 2014c).

2. Experimental programme

2.1 Test specimens and parameters examined

RC beam specimens having a rectangular cross section of 150×200 mm and a total length of 1200 mm (see Fig. 2a-b) were prepared. The geometry of the beams aims to simulate a member in flexure with a known lap splice length. The main bottom flexural reinforcement was spliced at the midspan zone and consisted of two steel bars of diameter d_b=12 and 16 mm. Two 50×100 mm notches were provided at the bottom of each beam to define the lap length and expose the main flexural reinforcement for measurements. The top beam reinforcement consisted of two continuous 10 mm bars. To prevent shear failure, 6 mm fully closed plain stirrups were placed at 100 mm centres outside the spliced zone. Due to the relatively short splice length selected for the beams (l_d=10d_b), the reinforcement is expected to remain elastic at failure. This splice length was considered sufficient to engage a significant number of bar ribs during bar movement.

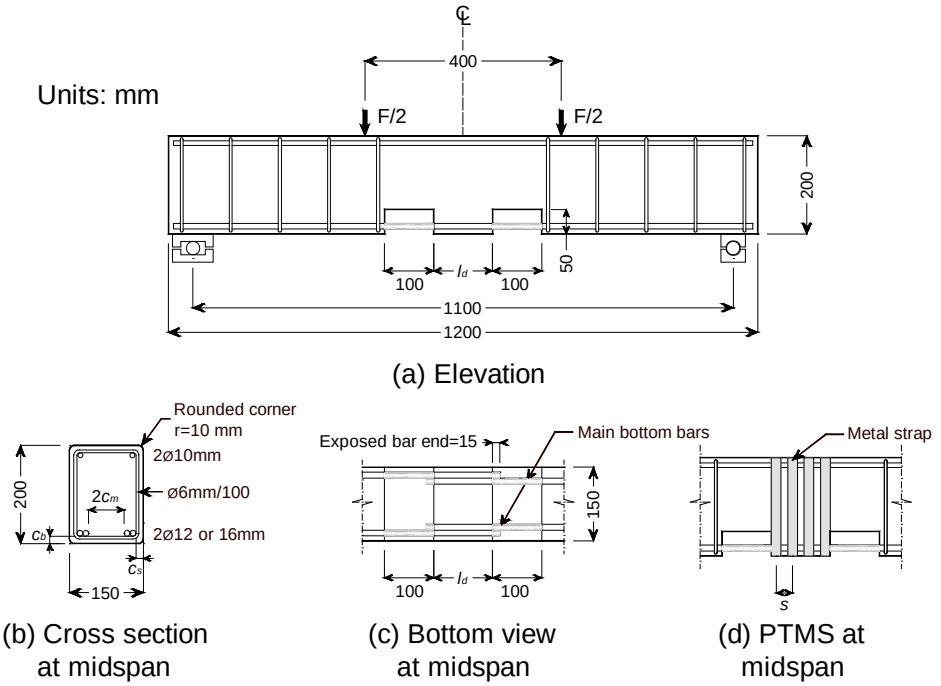

Fig. 2 Geometry and reinforcement details of beams

Table 1 summarises the main characteristics of the tested beams. To investigate different cover to bar diameter ratios (c/d_b), clear concrete covers of 10 and 20 mm were selected for the beams reinforced with 12 mm bars, whereas a 27 mm cover was used for the beams reinforced with 16 mm bars. These clear covers were selected to promote splitting along the spliced bars. The side (c_s) and bottom (c_b) covers of each beam were designed to be approximately similar. Different types and levels of confinement were investigated. The spliced zone of three beams was reinforced internally with two 6 mm steel stirrups at 70 mm centres. This led to confinement ratios $k_{tr}=A_{tr}/snd_b$ of 0.034 and 0.025 for the beams reinforced with d_b=12 and 16 mm bars, respectively, where A_{tr} is the cross-sectional area of the confinement, s is the spacing at stirrups centres, and n is the number of pairs of spliced bars (two for each tested beam). It should be noted that such relatively low k_{tr} values are typical of substandard RC columns of existing buildings in developing countries. To replicate substandard construction detailing, the stirrups were closed with 90° hooks instead of 135° typically required by current design provisions (e.g. ACI Committee 318 2011). Six beams were confined at the midspan zone using two layers of metal straps. The strap spacing at centres (s=25, 32 or 34 mm) was designed to provide approximate values of 1.5 and 2 times the confinement ratio of three counterpart beams confined with internal steel stirrups (see Table 1). These confinement ratios represent practical PTMS strengthening solutions for actual substandard RC components. Three unconfined beams with spliced bottom bars were also cast for comparison purposes as control specimens.

In Table 1, beams are identified according to the intended clear concrete cover c (SC10 for c=10 mm, SC20 for c=20 mm, and SC27 for c=27 mm), main bar diameter (12 or 16 mm) and type of confinement (Ctrl=unconfined control, S=internal steel stirrups, and PTMS=Post-Tensioned Metal Straps). Each beam group includes two PTMS-confined beams, which are identified by the last digit. The side (c_s), bottom (c_b) and internal (c_m) concrete covers (shown in Table 1) were measured after casting, according to the cover definitions shown in Fig. 2b. The measured covers produced c_{min}/d_b ratios ranged from 0.78 to 1.67 (c_{min} is the minimum of the concrete covers c_s, c_b and c_m).

Table 1 Main characteristics of tested beams

Group	Beam ID	f_{cm} (MPa)	Measured cover			Spliced bars	c_{min}/d_b	Confinement at midspan	Confinement ratio $k_{tr}=A_{tr}/snd_b$
			c_s	c_b	c_m				
SC10	SC10-D12-Ctrl	22.5	13	13	38	2 of 12 mm	1.08	None	-
	SC10-D12-S	22.5	12	12	39	2 of 12 mm	1.00	2 of 6 mm @ 70 mm	0.034
	SC10-D12-PTMS1	22.5	12	12	39	2 of 12 mm	1.00	4×2 layers @ 32 mm	0.053
	SC10-D12-PTMS2	37.2	17	12	34	2 of 12 mm	1.00	4×2 layers @ 32 mm	0.053
SC20	SC20-D12-Ctrl	37.2	17	17	34	2 of 12 mm	1.42	None	-
	SC20-D12-S	37.2	19	22	32	2 of 12 mm	1.58	2 of 6 mm @ 70 mm	0.034
	SC20-D12-PTMS1	37.2	20	24	31	2 of 12 mm	1.67	4×2 layers @ 32 mm	0.053
	SC20-D12-PTMS2	37.2	18	22	33	2 of 12 mm	1.50	5×2 layers @ 25 mm	0.067
SC27	SC27-D16-Ctrl	37.2	24	26	19	2 of 16 mm	0.78	None	-
	SC27-D16-S	37.2	26	25	17	2 of 16 mm	0.97	2 of 6 mm @ 70 mm	0.025
	SC27-D16-PTMS1	37.2	29	26	14	2 of 16 mm	0.97	5×2 layers @ 34 mm	0.037
	SC27-D16-PTMS2	37.2	22	27	21	2 of 16 mm	0.97	6×2 layers @ 25 mm	0.050

2.2 Material properties

Two batches of ready mixed normal-strength concrete were used to cast the beams. The concrete was produced using 10-mm maximum aggregate size, cement type OPC/GGBS (Ordinary Portland Cement/Ground-granulated blast-furnace slag) and a water cement ratio of 0.80. The fresh mixes had an average slump of 180 mm. The concrete was cast from the top of the beams so that the spliced bars are classified as "bottom cast bars". After casting, the beams were covered with wet hessian and polythene sheets, cured for seven days in the formwork and subsequently stored under standard laboratory conditions. Table 2 reports average 28-day results from cylinder tests for each concrete mix and corresponding standard deviations (SD). For each batch, the mean concrete compressive strength (f_{cm}) was obtained from tests on three 150×300 mm concrete cylinders according to EN 12390-3 (BSI 2009a). The indirect tensile splitting strength of concrete (f_{ctm}) was determined from tests on six 100×200 mm cylinders according to EN 12390-6 (BSI 2009b). All cylinders were cast at the same time and cured together with the beams.

Table 2 Properties of concrete (at 28 days) used to cast the beams

Test		Batch 1	Batch 2
Compressive strength (MPa)	Mean	22.5	37.2
	SD	1.67	1.28
Indirect tensile strength (MPa)	Mean	2.60	2.80
	SD	0.16	0.20

High-ductility Grade 500 ribbed bars were used as longitudinal top and bottom reinforcement for all beam specimens. The mechanical properties of the bars (shown in Table 3) were obtained from direct tension tests on three bar samples. For the 12 mm bar, average clear distances between the bar ribs and relative rib area were 8 mm and 0.084, respectively, whereas these values were 10 mm and 0.087 for the 16 mm bar. Commercially available high-strength high-ductility metal straps with nominal cross section 0.8×25 mm and corrosion-resistant surface coating were used as external PTMS confinement. Table 3 shows the mechanical properties of the steel straps obtained from three sample coupon tests.

Table 3 Average mechanical properties of reinforcing bars and metal straps

Nominal diameter, d_b (mm)	6	10	12	16	Straps 0.8×25mm
Yield strength, f_y (MPa)	360	533	470	470	760
Tensile strength, f_u (MPa)	420	688	570	570	1100
Yield strain, ε_y (%)	0.18	0.25	0.28	0.28	0.38
Elongation at maximum force, ε_u (%)	10.0	10.0	9.0	9.0	7.3[(a)]

[(a)] Corresponding value at the end of the yield plateau of the straps

Before applying the strapping, the corners at beam midspan were rounded off to a radius of approximately 10 mm to improve the effectiveness of the PTMS confinement (see Fig. 2b). All straps were post-tensioned using a compressed-air strapping tool set to an initial pressure of 6 bar, which led to a tensioning force in the straps of approximately 60-70% of their yield strength. It should be mentioned that most air tools using portable air compressors operate at pressures of 5-6 bar and therefore they can be easily used in practice. To maintain the post-tensioning force, the straps were fastened mechanically using 45 mm long push-type metal seals secured with a notch sealer (also powered by compressed air) using two notches (see Fig. 3). It should be mentioned that, during strap post-tensioning, some stress losses are expected in the straps due to friction between the straps and the concrete surface. However, previous test results (Moghaddam et al. 2010) indicate that the stress reduction due to friction is negligible (i.e. less than 10% loss).

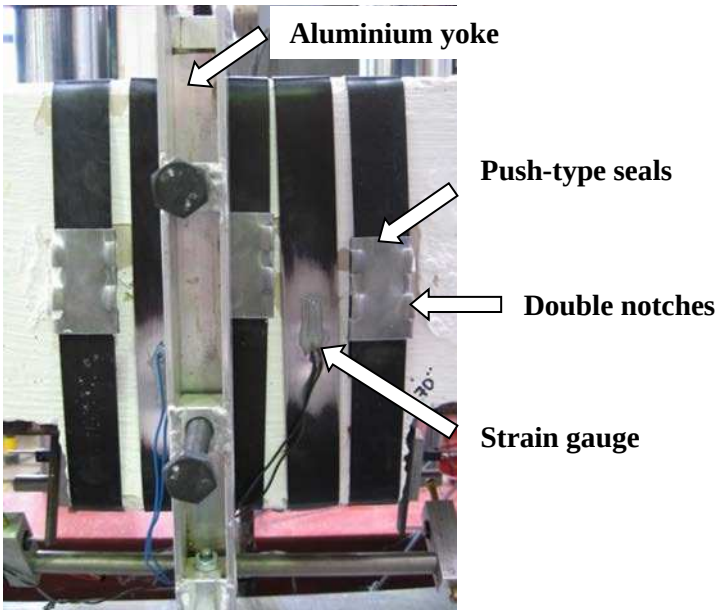

Fig. 3 View of metal straps and double-notched metal seals

2.3 Instrumentation and test set-up

All beams were tested in flexure using a four-column universal testing machine (UTM) with a capacity of 1,000 kN. The load was applied symmetrically through a stiff spreader loading beam as shown in Fig. 4a. The beams were simply supported over a clear span of 1100 mm. The load configuration (four-point bending) produced a constant moment over the spliced bars at midspan. A stiff steel H-section was used to support the concrete beams since the support platen of the UTM was slightly shorter than the clear span of the beams (see Fig. 4a).

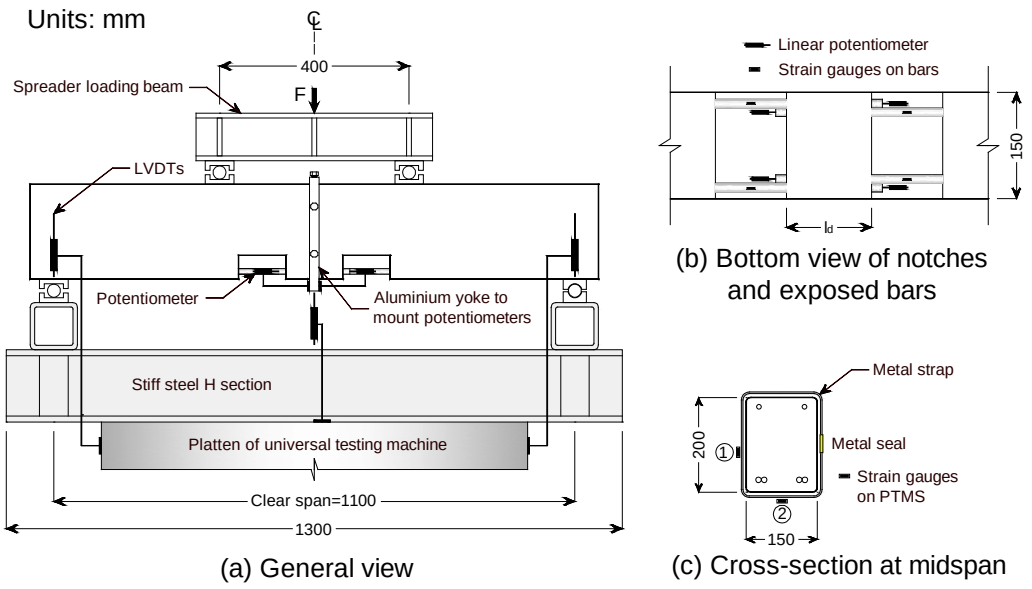

Fig. 4 Typical test set-up and instrumentation

Vertical deflections at the beam centreline were measured using two Linear Variable Displacement Transducers (LVDTs), one on each beam sides. To compute net deflections, vertical displacements at the supports were also monitored using two LVDTs. The free-end slip of the spliced bars was monitored using four electrical linear potentiometers measuring to a precision of 1×10^{-4} mm and with expected errors of ±1%. These potentiometers were mounted on an aluminium yoke. The yoke was clamped at the centreline of the beam to record bar slippage relative to the intact concrete, as shown in Fig. 4a (see also Fig. 3 where the actual aluminium yoke is shown at the middle of the beam). The strains of the spliced bars were measured using four electrical resistance strain gauges fixed to the bars exposed at the notches (see Fig. 4b). Additional strain gauges were fixed on the metal straps to monitor the strains developed in the external confinement during the post-tensioning process and testing (see location in Fig. 3 and Fig. 4c).

The tests were carried out in displacement control at a loading rate of 0.10 mm/min. An initial load cycle of 10 kN was applied and then released to check the measuring equipment and release residual stresses in the beams. For the control beams, the load was then restored and increased gradually up to the maximum beam capacity. After this point, the confined beams were subjected to four full load-reload cycles (with the exception of beams SC10-D12-S and SC10-D12-PTMS1). The formation and development of cracks were monitored continuously during the tests. The tests were halted when splitting failure occurred (in unconfined beams), or when the bar slip was similar to the bar rib spacing (in confined beams).

3. Experimental results and discussion

Table 4 reports the maximum capacity F_{max} of the tested beams and the corresponding midspan deflection δ_m at F_{max}. It also shows the increase of capacity (ΔF) and deflection ($\Delta\delta_m$) of confined beams compared to the corresponding unconfined control specimen, as well as the deflection ratio $\delta_{70\%}/\delta_m$, where $\delta_{70\%}$ is the beam deflection after a 30% drop of F_{max} (i.e. after maximum load). To account for the effect of different concrete strengths and

compare the experimental results, the capacities F_n for Group SC10 are normalised to a common concrete strength of 37.2 MPa by multiplying F_{max} by $(37.2/f_{cm})^{1/4}$, as suggested by Hamad and Rteil (2006), where f_{cm} is the corresponding concrete strength of the beam. The following sections summarise the most significant observations of the testing programme and discuss the results.

Table 4 Load and deflection results of tested beams

Group	Beam ID	F_{max} (kN)	F_n (kN)	δ_m (mm)	ΔF (%)	$\Delta\delta_m$ (%)	$\delta_{70\%}/\delta_m$ (-)
SC10	SC10-D12-Ctrl	33	37[(a)]	1.14	-	-	0
	SC10-D12-S	37	42[(a)]	1.52	+12	+33	2.3
	SC10-D12-PTMS1	47	53[(a)]	1.68	+42	+47	2.3
	SC10-D12-PTMS2	48	48	1.67	+30	+47	2.6
SC20	SC20-D12-Ctrl	35	35	1.22	-	-	0
	SC20-D12-S	39	39	1.82	+11	+49	0
	SC20-D12-PTMS1	54	54	2.40	+54	+96	2.3
	SC20-D12-PTMS2	58	58	2.54	+66	+108	1.7
SC27	SC27-D16-Ctrl	52	52	1.28	-	-	0
	SC27-D16-S	51	51	2.08	-2	+63	2.7
	SC27-D16-PTMS1	74	74	5.14	+42	+302	5.5
	SC27-D16-PTMS2	80	80	7.36	+54	+475	7.0

[(a)] Value normalised by $(37.2/f_{cm})^{1/4}$

3.1 Failure mode

In all beams, first flexural cracks developed at the internal corners of the notches, just outside the splice zone. As the load increased in the unconfined beams, horizontal side and bottom splitting cracks developed suddenly along the splice, followed by a sudden drop of capacity. This was accompanied by an explosive noise and the detachment of the cover, as shown in Fig. 5a. After failure, only the top beam reinforcement prevented the beams' collapse.

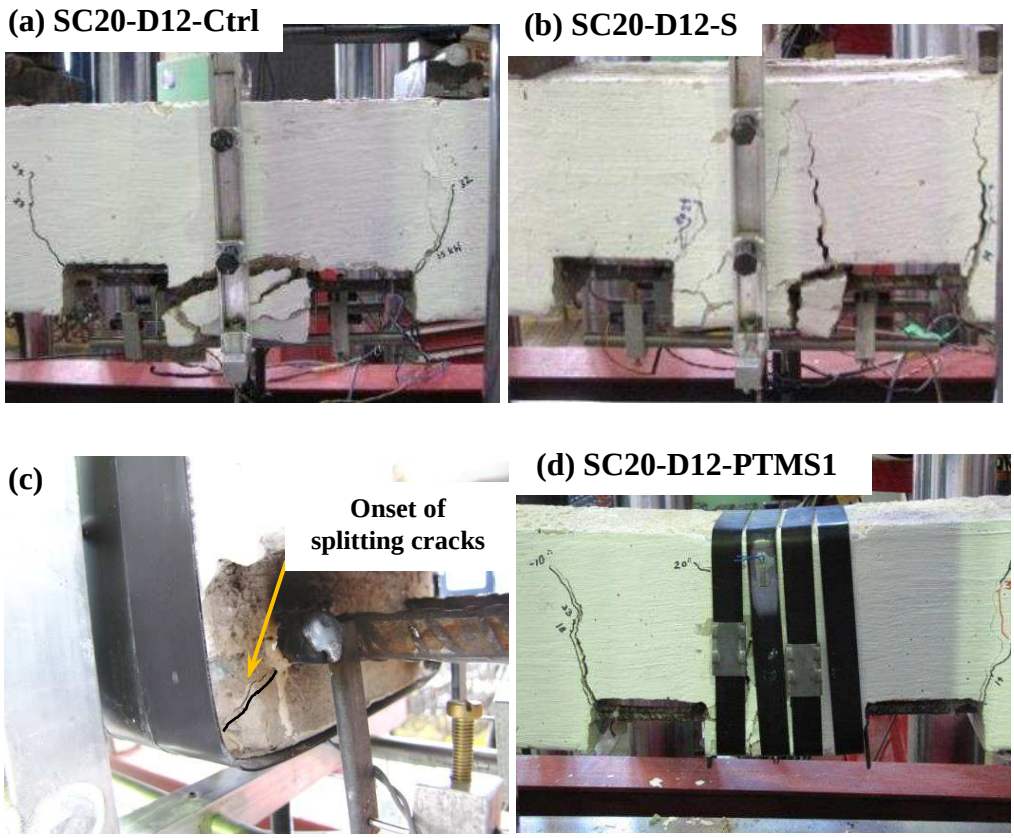

Fig. 5 Typical failures at the midspan of beams (a) unconfined control, (b) steel-confined, (c) onset of splitting cracks in PTMS-confined beams (crack highlighted), and (d) typical failure of PTMS-confined beams

The use of internal stirrups in the splice zone did not delay the onset of flexural cracking of the steel-confined beams. However, unlike the unconfined beams, additional flexural cracks formed across the constant moment region. Splitting cracks developed along the spliced bars when the load approached maximum capacity. Fig. 5b shows a typical failure of a steel-confined beam. Although the concrete cover did not spall completely, large flexural and splitting cracks appeared across the spliced zone.

The initial flexural cracks for PTMS-confined beams also developed at the internal corners of the notches. However, the splitting developed at the confined corners of the midspan tension zone (see Fig. 5c). This was followed by the development of new splitting cracks. For the beam Groups SC10 and SC20, such splitting cracks formed at the side and bottom concrete covers. Conversely, for beam Group SC27, concrete splitting occurred first between the spliced bars, and

then at the side and bottom covers. This was due to the small internal concrete cover between the spliced bars of the SC27 beams (see c_m values in Table 1). The PTMS confinement controlled the splitting crack opening and prevented concrete cover spalling during the tests. Fig. 5d shows a typical PTMS-confined beam at failure. Although a few metal seals experienced local shearing-off, no damage was evident on the metal straps. After the removal of the metal straps, it was confirmed that extensive splitting cracks developed within the midspan zone

3.2 Load-deflection relationships

Fig. 6 shows the load-deflection relationships obtained for the three beam Groups. In Fig. 6a-c, the sudden failure of the unconfined beams is indicated by a star symbol. It is seen that the use of internal stirrups at the spliced zone led to a less brittle response, characterised by a gradual drop in load capacity after the maximum load. The deflections at splitting of the steel-confined beams (beam SC27-D16-S) increased by up to 63% when compared to their unconfined counterparts (see $\Delta\delta_m$ in Table 4). However, the load capacity of steel-confined beams was similar to or slightly higher (up to 12%) than that of the unconfined beams. Note that the experimental response of beam SC20-D12-S (Fig. 6b) was recorded only up to approximately δ_m=2 mm.

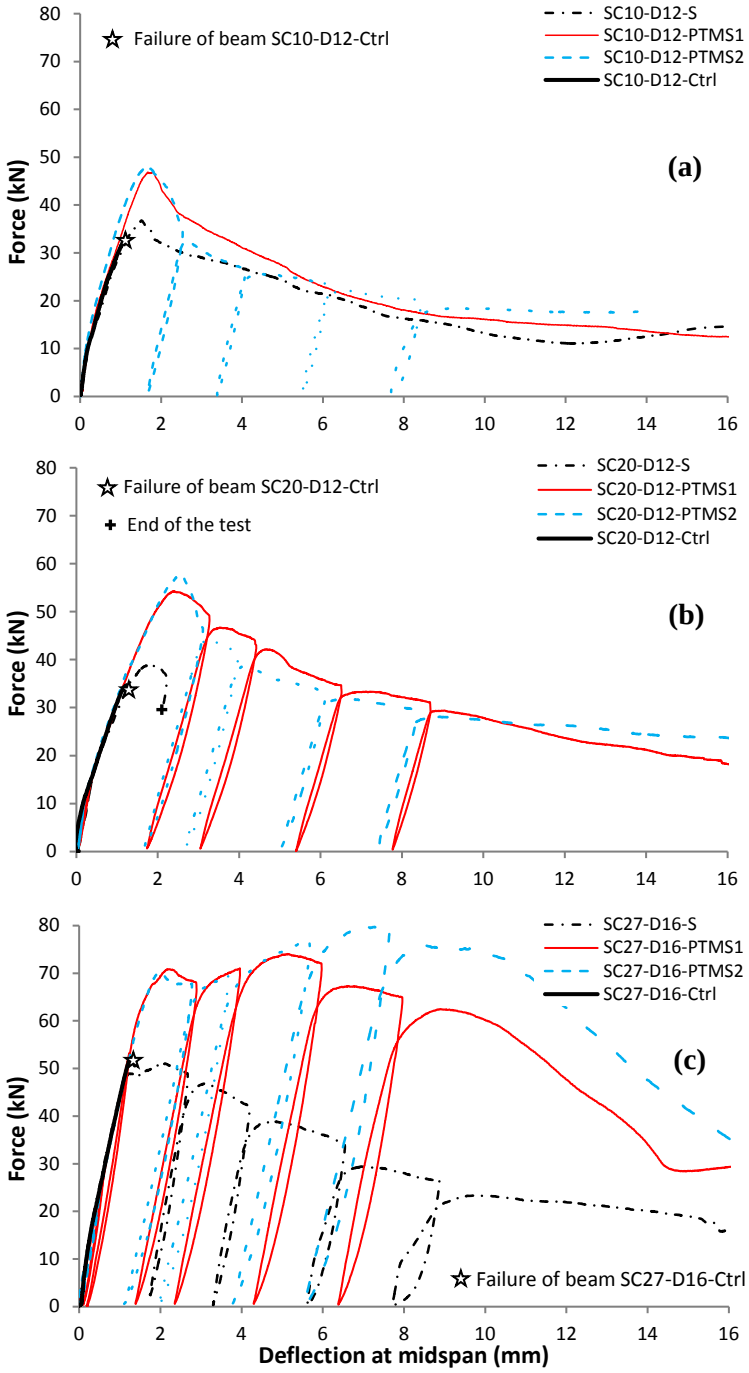

Fig. 6 Load-midspan deflection response of beam Groups (a) SC10, (b) SC20, and (c) SC27 (actual experimental response)

Overall, the results in Fig. 6a-c show that the use of PTMS confinement was very effective at improving the load-deflection behaviour of the beams by delaying splitting failure. All PTMS-confined specimens had higher load capacities and larger deflections in comparison to their unconfined and internally steel-confined counterparts. As shown in Table 4, the capacity of PTMS-confined specimens increased by up to 66% and 55% with reference to the unconfined and steel-confined specimens, respectively. The use of PTMS confinement also increased

the deflection at splitting failure by up to 475% (beam SC27-D16-PTMS2) compared to the unconfined control beam specimens. Following splitting, after a drop of 30% in capacity, the deflections were up to 260% larger than those of steel-confined specimens. As expected, the results indicate that the enhancement in the load-deflection response was more evident for specimens with higher confinement ratios provided by the external PTMS.

3.3 Bond-slip response of spliced bars

To assess the effect of confinement at midspan, bond-slip relationships of the spliced bars are examined using the test results. The average bond stress τ of a bar in tension is calculated assuming that bond is uniformly distributed over the lap length l_d, according to Equation (1):

$$\tau = \frac{\varepsilon_s E_s d_b}{4 l_d} \qquad (1)$$

where ε_s is the average bar strain (from the four gauges shown in Fig. 4b), E_s is the elastic modulus of the bars (E_s=200 GPa), and the rest of the variables are as defined before. Bar slip was obtained from the average readings of the linear potentiometers located at the exposed free ends of the bars, as shown in Fig. 4b. Threfore, the measured free end slips do not include the bar elongation along the splice.

Fig. 7 shows the bond-slip relationships for all beam specimens. The bond-slip relationships of the two splices were similar for each tested beam and therefore average results are shown. Overall, the bond-slip curves are consistent with the corresponding load-deflection responses shown in Fig. 6a-c, which confirms that the beam failure mainly depends on the bond behaviour of the spliced bars. The slight differences between load-deflection and bond-slip curves may be attributed to minor variations of the effective beam depths.

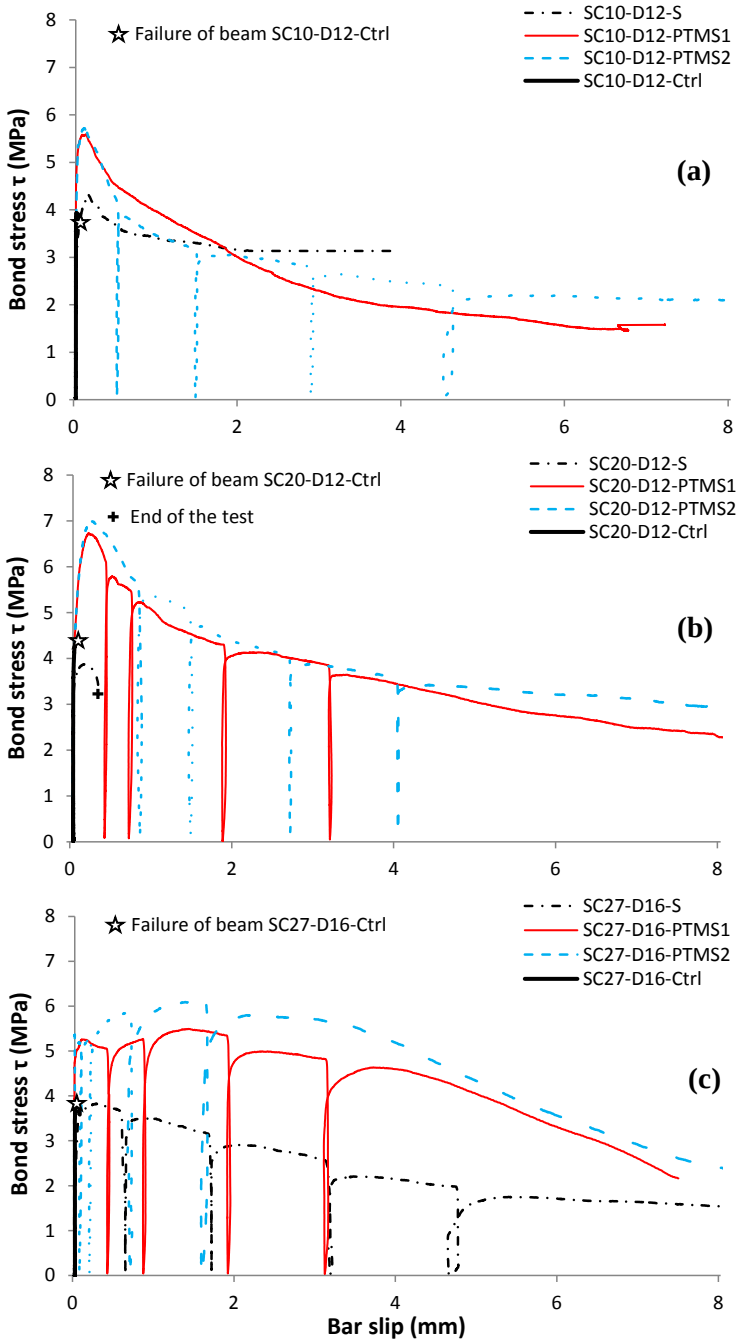

Fig. 7 Bond-slip response of beam Groups (a) SC10, (b) SC20, and (c) SC27 (actual experimental response)

It is shown in Fig. 7a-c that, during the initial loading stages, the bond-slip relationships of all beams were similar and bar slip was negligible. Concrete cover splitting started at bond stresses of approximately 70-80% the bond splitting strength, and this was accompanied by the onset of significant bar slippage. After splitting and for the same slip value, the bond stresses developed by the PTMS-confined beams were consistently larger than the unconfined and steel-confined beams, due to the restraining effect of the straps which limited splitting crack

propagation. The bond stress curves levelled off at slips of approximately 8 mm, which corresponds to the bar rib spacing. The splices had a relatively low residual bond stress at the end of the tests (40-50% of the peak bond capacity).

Table 5 summarises the results obtained at the peak capacity of each beam: experimental bar stress f_s, average bond strength τ calculated using Equation (1), normalised bond strength $\tau_n=\tau\cdot(37.2/f_{cm})^{1/4}$, free-end slip of the spliced bars s_e, bond ratio τ_n/τ_{Ctrl}, (where τ_{Ctrl} is the bond strength of the control specimen of each beam Group), and strains in the PTMS confinement ε_{strap}. The bar stresses f_s indicate that, as expected, the reinforcement remained elastic up to failure due to the relatively short lap splice length used for the tested beams (lap length $l_b=10d_b$). Even though the bond strength of the steel-confined beams was slightly lower or higher than that of the unconfined beams, the use of steel stirrups increased, on average, the bar slip at failure by 5 times. The lower bond strength of beams SC20-D12-S and SC27-D16-S can be attributed to the relatively high variability of concrete in tension, which may have caused early failures in such beams compared to the control counterparts. In general, however, bond strength is expected to increase with the amount of confinement.

Table 5 Bar stresses and bond-slip results of tested beams

Group	Beam ID	f_s (MPa)	τ (MPa)	τ_n (MPa)	s_e (mm)	τ_n/τ_{Ctrl} (-)	ε_{strap} (%)
SC10	SC10-D12-Ctrl	155	3.80[(a)]	4.31[(b)]	0.05	1.00	-
	SC10-D12-S	170	4.33	4.91	0.19	1.14	-
	SC10-D12-PTMS1	221	5.53	6.27	0.09	1.46	0.32
	SC10-D12-PTMS2	230	5.75	5.75	0.11	1.33	0.31
SC20	SC20-D12-Ctrl	177	4.41[(a)]	4.41	0.04	1.00	-
	SC20-D12-S	155	3.87	3.87	0.14	0.88	-
	SC20-D12-PTMS1	268	6.71	6.71	0.19	1.07	0.26
	SC20-D12-PTMS2	279	6.97	6.97	0.22	1.58	0.28
SC27	SC27-D16-Ctrl	161	4.03[(a)]	4.03	0.03	1.00	-
	SC27-D16-S	153	3.82	3.82	0.28	0.95	-
	SC27-D16-PTMS1	219	5.49	5.49	1.41	1.36	0.30
	SC27-D16-PTMS2	248	6.21	6.21	1.50	1.54	0.33

[(a)] Unconfined bond strength τ_{Ctrl} of the group

[(b)] Unconfined bond strength τ_{Ctrl} for beam SC10-D12-PTMS2 only

The results in Table 5 highlight the effectiveness of active PTMS confinement at improving the bond-slip behaviour of the reinforcement. Compared to unconfined specimens, the bond strength was enhanced by up to 58% for PTMS-confined beams (SC20-D12-PTMS2). The premature failure of the unconfined control beams was mainly due to concrete cover spalling at very low bar slip values (0.03 to 0.05 mm). The PTMS confinement resulted in an increased slip at peak load of at least 80%. As it was discussed before, the effect of confinement was more evident in Group SC27, where larger side covers were used (see Table 5). Overall, all PTMS-confined beams experienced a splitting-induced pullout failure. As a result, the use of larger PTMS confinement ratios is not expected to improve significantly the bond-slip behaviour of the spliced bars.

The test results of this study suggest that the PTMS confinement can be as effective as other techniques currently used in practical strengthening solutions. For instance, the average lap bond strength enhancement attained in the PTMS-confined beams was 39%, which is comparable to an average bond enhancement of 41% observed in beams confined with CFRP sheets at the midspan zone and tested under similar conditions (Garcia et al. 2013). Compared to FRP, PTMS can be rapidly applied to provide active confinement at a lower material cost, but the effectiveness of the technique can be further improved by preventing local damage in the metal seals as discussed in the following section. Conversely, FRP sheets are an effective passive confinement solution for short lap splices (e.g. Garcia et al. 2013, 2014b), but the application of FRP requires a thorough surface preparation and skilled technical staff.

3.4 Development of strains in PTMS confinement

To assess the force applied by the external PTMS confinement, the stress in the metal straps was monitored using two strain gauges. Fig. 8 shows the location of the strain gauges and the corresponding development of strains in the metal straps during the test on beam SC20-D12-PTMS1. These are typical results and the following observations apply to all PTMS-confined beams. As shown in Fig. 8, the initial PTMS strains were 2600-2800 με, which indicates that the post-

tensioning force applied before the tests developed approximately 70% of the strap yielding stress. These strains remained relatively constant during the initial loading and up to approximately 70-80% of the peak bond capacity, when splitting cracks formed along the splices. Following splitting, the PTMS strains reduced progressively partly to some local damage of the push-type seals, thus resulting in some stress relaxation in the straps. Despite this loss of post-tensioning force, the straps maintained 80% of their initial force until the end of the tests. Additional tests are necessary to examine the post-tensioning losses and overall long-term behaviour of the PTMS strengthening technique.

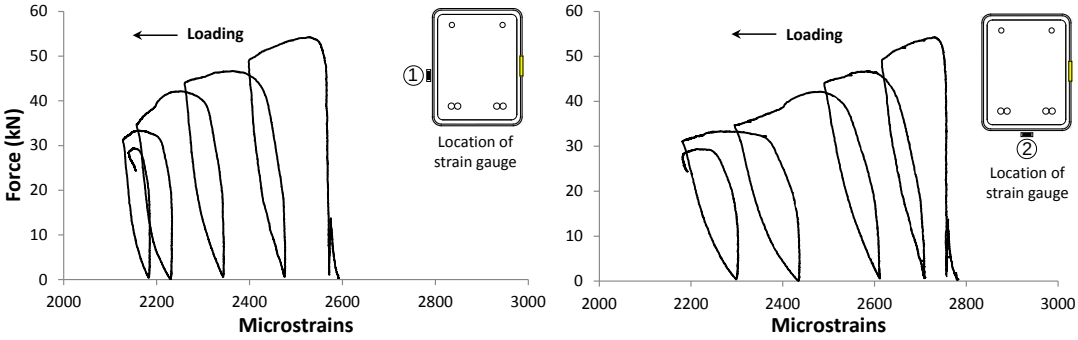

Fig. 8 Typical development of strains in metal straps (beam SC20-D12-PTMS2)

4. Bond strength model proposal

Table 6 compares the experimental bond strength enhancement (τ_{PTMS}) of the PTMS-confined beams with predictions of existing models ($\tau_{PTMS,p}$) (Orangun et al. 1977; Zuo and Darwin 2000; Harajli 2009; ACI Committee 408 2012; fib 2013). To assess the accuracy of the models, the Test/Prediction ratios (T/P) and corresponding standard deviations (SD) are also reported. For each group, the values τ_{PTMS} were estimated as the difference between the bond strength of the PTMS-confined beams and the unconfined control specimen, i.e. $\tau_{PTMS}=\tau-\tau_{Ctrl}$ (except for beam SC10-D12-PTMS2, where τ_{Ctrl} was taken as τ_n). It is assumed that the total bond strength of a short splice (τ) is the additive contribution of the concrete cover (τ_{Ctrl}) and the PTMS confinement (τ_{PTMS}), i.e. $\tau=\tau_{Ctrl}+\tau_{PTMS}$. The values τ and τ_{Ctrl} were obtained directly from the experimental results listed in Table 5.

Table 6 Predictions of experimental bond strength of PTMS-confined beams obtained using existing models

Beam	Test τ_{PTMS} (MPa)	Orangun et al. (1977)		Zuo and Darwin (2000)		Harajli (2009)		ACI Committee 408 (2012)		*fib* Model Code 2010 (2013)	
		$\tau_{PTMS,p}$ (MPa)	T/P	$\tau_{PTMS,p}$ (MPa)	T/P	$\tau_{PTMS,p}$ (MPa)	T/P	$\tau_{PTMS,p}$ (MPa)	T/P	$\tau_{PTMS,p}$ (MPa)	T/P
SC10-D12-PTMS1	1.73	1.19	1.46	2.74	0.63	1.07	1.61	2.30	0.75	3.41	0.51
SC10-D12-PTMS2	1.44	1.52	0.95	3.99	0.36	1.38	1.04	3.35	0.43	3.87	0.37
SC20-D12-PTMS1	2.30	1.52	1.51	3.99	0.58	1.97	1.17	3.35	0.68	3.87	0.59
SC20-D12-PTMS2	2.56	1.52	1.68	4.37	0.59	2.69	0.95	3.73	0.69	4.90	0.52
SC27-D16-PTMS1	1.46	1.52	0.96	2.71	0.54	0.90	1.61	2.35	0.62	2.57	0.57
SC27-D16-PTMS2	2.18	1.52	1.43	2.97	0.73	1.30	1.67	2.61	0.84	3.47	0.63
Mean			1.33		0.57		1.34		0.67		0.53
SD			0.28		0.11		0.30		0.13		0.09

The results in Table 6 indicate that the existing models, in general, do not predict accurately the bond strength enhancement due the PTMS confinement, with Orangun et al. and Harajli equations showing the largest scatter (SD=0.28 and 0.30, respectively). Moreover, most of the examined models overestimate the bond strength enhancement due to the PTMS confinement. This is particularly evident for Zuo and Darwin model, which overestimates the bond results by a factor of up to 2.8 (beam SC10-D12-PTMS2).

Based on the above observations, a new model is proposed to predict more accurately the bond strength enhancement of short splices due to PTMS confinement using the results of this study. The proposed model considers the concrete around the lap spliced bars as 'confined cylinders' of thickness c_{min} subjected to corner confining forces P_s as shown in Fig. 9a, where side cover splitting is considered.

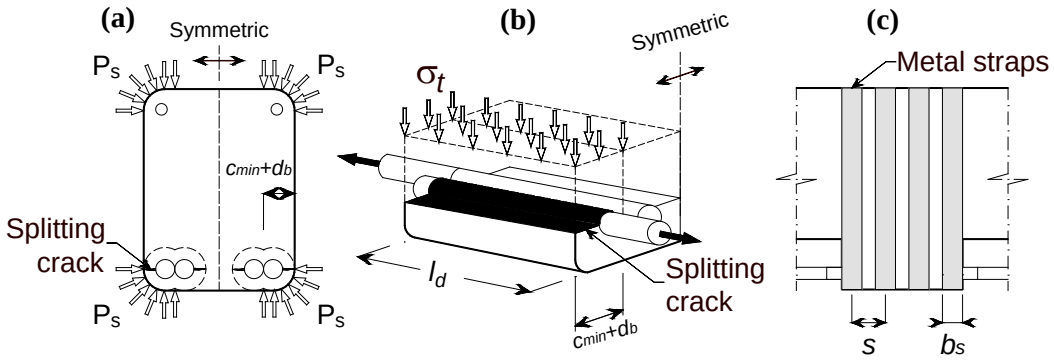

Fig. 9 Confining stresses from PTMS on a splitting crack (assuming $s \leq 1.30 b_s$)

The proposed model considers the effect of the PTMS confinement through an additional confining stress σ_t acting over a split plane of width $c_{min}+d_b$ (see Fig. 9b). Assuming that the spliced bar slips when the pulling force in the bar exceeds the friction applied by σ_t over the split area $(c_{min}+d_b)\cdot l_d$, the confining stress σ_t applied over one lap spliced bar can be calculated as:

$$\sigma_t = \frac{P_s}{b_s\left(c_{\min}+d_b\right)} = \frac{f_p \cdot t}{\left(c_{\min}+d_b\right)} \qquad (2)$$

where P_s is the force in the metal strap and is defined as $P_s=f_p\cdot t\cdot b_s$ (b_s and t are the strap width and strap thickness, respectively, see Fig. 9c), and f_p is the strap stress. Note that Equation (2) assumes that the metal straps are closely spaced (i.e. that

$s \leq 1.30 b_s$) and, therefore, the confining stress σ_t is considered to be uniform along the splice length.

To assess the contribution of PTMS confinement to the bond strength τ_{PTMS}, the influence of the parameters examined in the tests is investigated. Previous research has shown that f_{cm}, f_p and the ratios l_d/d_b and c_{min}/d_b have a strong influence on bond strength (e.g. Orangun et al. 1977; fib 2013). The results from the six beams tested in this study (Table 1) and from six additional RC beams with lap splices of $l_d=25d_b$ confined with PTMS tested under similar conditions (Helal 2012) were used to evaluate the bond strength enhancement due to PTMS confinement (τ_{PTMS}). Based on these results, the following general equation is proposed.

$$\frac{\tau_{PTMS}}{(f_{cm})^p} = A\sigma_t \cdot \left[1 + \left(B\frac{d_b}{l_d} - C\right)\frac{c_{\min}}{d_b} + D\frac{l_d}{d_b}\right] \quad (3)$$

Based on nonlinear regression analysis and through iterations using a least square error approach, the constant parameters A, B, C and D in the above equation were calculated as 1/456, 150, 12.6 and 2/3, respectively. The power factor p=1/4 was also found to represent adequately the effect of concrete tensile strength on τ_{PTMS} as shown in Fig. 10. The PTMS-confined beams with lap splices of $l_d=25d_b$ are represented with "×" symbols in Fig. 10

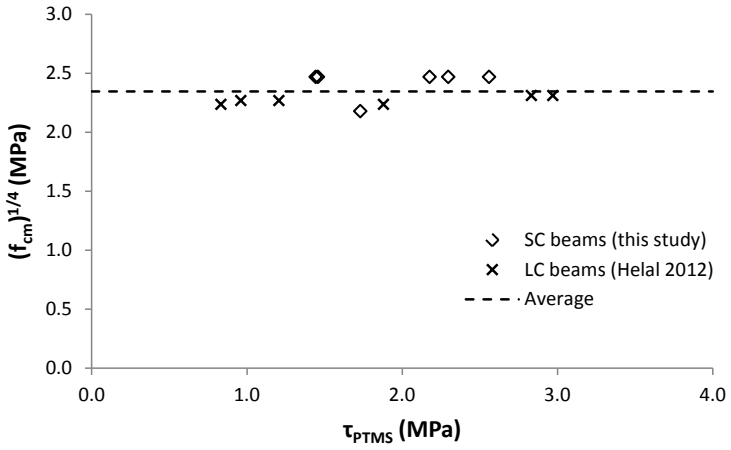

Fig. 10 Normalisation of τ_{PTMS} to $(f_{cm})^{1/4}$

Therefore, Equation (3) can be rewritten as follows to calculate the bond strength enhancement due to PTMS confinement:

$$\frac{\tau_{PTMS}}{(f_{cm})^{1/4}} = \frac{N \cdot f_p \cdot t}{456 \cdot n(c_{\min} + d_b)} \cdot \left[1 + \left(150\frac{d_b}{l_d} - 12.6\right)\frac{c_{\min}}{d_b} + \frac{2}{3}\frac{l_d}{d_b}\right] \quad (4)$$

where N is the number of metal straps across the lap length l_d, n is the total number of splices in the tension side of the cross section (which accounts for the number of developed cracks), and the rest of the variables are as defined before.

Fig. 11 compares the test results with the predictions given by Equation (4). The figure also shows a straight line based on the regression analyses of the test data points, the corresponding 95% confidence band (dotted-line hyperbolas), and a 45° line which indicates a perfect coincidence of test results and predictions. It is shown that the proposed equation predicts the test results with good accuracy as most of the data points are close to the 45° line. The use of Equation (4) leads to a mean Test/Prediction ratio of 0.94 and relatively low scatter (SD=0.18) with the 45° line lying completely within the 95% confidence band, thus indicating that Equation (4) accounts adequately for the parameters influencing the response. Therefore, Equation (4) can be used for assessment and strengthening of short splices in RC buildings. As the performance of Equation (4) was only validated for values c_{min}/d_b ranging from 0.8 to 1.7, further research is necessary to validate its applicability to other cases.

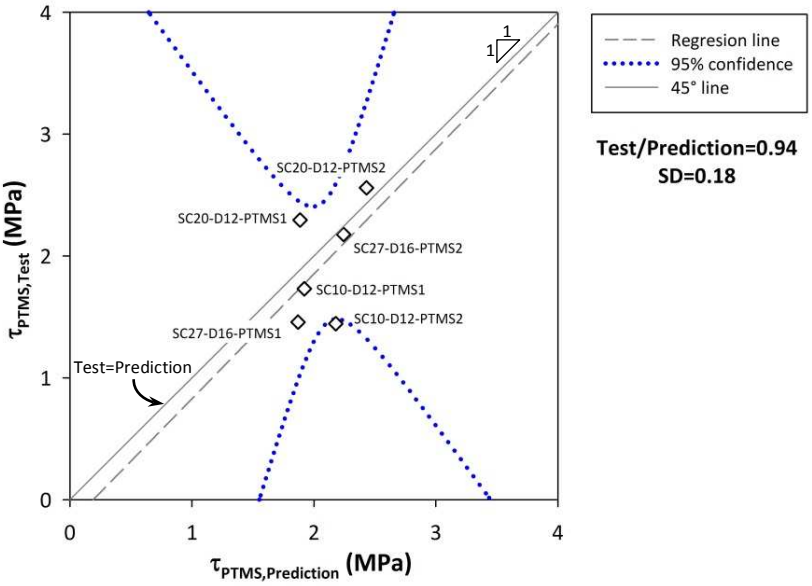

Fig. 11 (a) Comparison of predictions given by Equation (4) and test results

It should be noted that whilst the bond enhancement due to steel confinement has been frequently normalised to $(f_{cm})^{1/2}$ or $(f_{cm})^{3/4}$ to consider the effect of concrete

tensile strength (e.g. Orangun et al. 1977; Harajli 2009), Equation (4) normalises τ_{PTMS} to $(f_{cm})^{1/4}$ as this value leads to lower scatter of results (Helal 2012). However, further data test are necessary to verify the accuracy of such normalisation. To compute the total bond strength of the spliced bars, the result from Equation (4) has to be added to the concrete contribution (τ_{Ctrl}). The total bond strength of a short splice ($\tau_{Ctrl}+\tau_{PTMS}$) should be limited to the bond strength mobilised at bar pullout τ_0. Based on recent results from a comprehensive study on bond behaviour of steel bars (Harajli 2009), it is suggested to adopt $\tau<\tau_0=2.57(f_{cm})^{1/2}$.

5. Conclusions

This paper presents results from short splices in RC beams confined with a novel technique using Post-Tensioned Metal Straps (PTMS). The beams were subjected to four-point bending and were designed to fail by bond-splitting at midspan, where the main flexural reinforcement was lap spliced for a short length (10 bar diameters). Based on the results, the following conclusions can be drawn:

1) Unconfined control beams with short splices failed in a brittle manner due to splitting of the concrete cover around the splice. For the tested beams, bar slip at splitting ranged from 0.03 to 0.05 mm.

2) In comparison to unconfined specimens, steel-confined beams failed by splitting at similar or slightly higher loads (by up to 12%) and bond strengths (by up to 14%). However, steel-confinement increased bar slips on average by 5 times. Following splitting, steel-confined beams showed a less brittle behaviour and sustained significant additional deformations accompanied by a gradual drop in capacity.

3) The use of external PTMS confinement delayed the splitting failure of the lap splices. In comparison to unconfined specimens, the PTMS confinement also enhanced the bond strength by up to 58%, while the bar slip at splitting failure increased by at least 80%.

4) Local progressive damage in the push-type seals reduced the initial post-tensioning force in the metal straps by approximately 20%. The PTMS locking system is found to be reliable, since the tension losses mainly occurred towards the end of the tests where the specimens were extensively damaged. Despite the losses observed in the straps, the proposed PTMS strengthening technique was extremely effective at maintaining the integrity of the beams even after severe splitting occurred.

5) Based on the test data, a model is proposed to predict the bond strength enhancement of short splices due to active PTMS confinement. This can be used for assessment and strengthening of short splices in substandard RC structures. However, more research is required to verify the applicability of the proposed model for PTMS strengthening of elements where bar yielding can occur.

6) The experimental results of this study indicate the PTMS confinement is very effective to enhance the behaviour of RC elements subjected to 'monotonic' unidirectional load. However, further tests are necessary to validate the effectiveness of this technique as well as potential strap post-tensioning losses in elements subjected to fully reversed cyclic loading.

References

Aboutaha RS, Engelhardt MD, Jirsa JO, Kreger ME (1996) Retrofit of concrete columns with inadequate lap splices by the use of rectangular steel jackets. Earthq Spectra 12 (4):693-714

ACI Committee 318 (2011) ACI 318-11 Building Code Requirements for Structural Concrete and Commentary. American Concrete Institute, Farmington Hills, MI; .

ACI Committee 408 (2012) 408R-03 Bond and Development of Straight Reinforcing Bars in Tension (Reapproved 2012). American Concrete Institute. Farmington Hill, MI

Ahmed S (2011) Seismic vulnerability of non-ductile reinforced concrete structures in developing countries. Ph.D. thesis, Dept. of Civil and Structural Engineering, The University of Sheffield, UK

Beschi C, Meda A, Riva P (2011) Column and Joint Retrofitting with High Performance Fiber Reinforced Concrete Jacketing. Journal of Earthquake Engineering 15 (7):989-1014. doi:Doi 10.1080/13632469.2011.552167

Bournas DA, Triantafillou TC (2011) Bond strength of lap-spliced bars in concrete confined with composite jackets. J Compos Constr 15 (2):156-167. doi:10.1061/(ASCE)CC.1943-5614.0000078

Bousias S, Spathis AL, Fardis MN (2007) Seismic retrofitting of columns with lap spliced smooth bars through FRP or concrete jackets. J Earthquake Eng 11 (5):653-674. doi:10.1080/13632460601125714

Breña SF, Schlick BM (2007) Hysteretic behavior of bridge columns with FRP-jacketed lap splices designed for moderate ductility enhancement. J Compos Constr 11 (6):565-574. doi:10.1061/(Asce)1090-0268(2007)11:6(565)

BSI (2009a) BS EN 12390-3:2009 Testing hardened concrete Part 3: Compressive strength of test specimens. British Satandards Institution, London, UK, .

BSI (2009b) BS EN 12390-6:2009 Testing hardened concrete Part 6: Tensile splitting strength of test specimens. British Satandards Institution, London, UK, .

Cairns J (2014) Staggered lap joints for tension reinforcement. Struct Concrete 15 (1):45-54. doi:DOI 10.1002/suco.201300041

Chai YH, Priestley MJN, Seible F (1991) Seismic retrofit of circular bridge columns for enhanced flexural performance. Aci Struct J 88 (5):572-584

Coffman HL, Marsh ML, Brown CB (1993) Seismic durability of retrofitted reinforced-concrete columns. J Struct Eng-Asce 119 (5):1643-1661. doi:10.1061/(ASCE)0733-9445(1993)119:5(1643)

ElGawady M, Endeshaw M, McLean D, Sack R (2010) Retrofitting of rectangular columns with deficient lap splices. J Compos Constr 14 (1):22-35. doi:Doi 10.1061/(Asce)Cc.1943-5614.0000047

fib (2000) Bulletin 10 Bond of reinforcement in concrete - State-of-art report. Fédération Internationale du Béton, Lausanne, Switzerland; .

fib (2013) Model Code for Concrete Structures 2010. 1st edn. Ernst & Sohn GmbH & Co, Berlin, Germany

Frangou M, Pilakoutas K, Dritsos S (1995) Structural Repair Strengthening of RC Columns. Construction and Building Materials 9 (5):259-266. doi:Doi 10.1016/0950-0618(95)00013-6

Gambarova PG, Rosati GP (1997) Bond and splitting in bar pull-out: Behavioural laws and concrete cover role. Mag Concrete Res 49 (179):99-110

Garcia R, Hajirasouliha I, Guadagnini M, Helal Y, Jemaa Y, Pilakoutas K, Mongabure P, Chrysostomou C, Kyriakides N, Ilki A, Budescu M, Taranu N, Ciupala MA, Torres L, Saiidi M (2014a) Full-scale shaking table tests on a substandard RC building repaired and strengthened with Post-Tensioned Metal Straps. J Earthquake Eng 18 (2):187-213. doi:10.1080/13632469.2013.847874

Garcia R, Hajirasouliha I, Pilakoutas K (2010) Seismic behaviour of deficient RC frames strengthened with CFRP composites. Eng Struct 32 (10):3075-3085. doi:DOI 10.1016/j.engstruct.2010.05.026

Garcia R, Helal Y, Pilakoutas K, Guadagnini M (2013) Bond strength of short lap splices in RC beams confined with steel stirrups or external CFRP. Mater Struct:1-17

Garcia R, Helal Y, Pilakoutas K, Guadagnini M (2014b) Bond behaviour of substandard splices in RC beams externally confined with CFRP. Construction and Building Materials 50:340-351

Garcia R, Jemaa Y, Helal Y, Guadagnini M, Pilakoutas K (2014c) Seismic strengthening of severely damaged beam-column RC joints using CFRP. J Compos Constr 18 (2):04013048. doi:10.1061/(ASCE)CC.1943-5614.0000448

Hamad BS, Rteil AA (2006) Comparison of roles of FRP sheets, stirrups, and steel fibers in confining bond critical regions. J Compos Constr 10 (4):330-336. doi:10.1061/(Asce)1090-0268(2006)10:4(330)

Harajli MH (2006) Effect of confinement using steel, FRC, or FRP on the bond stress-slip response of steel bars under cyclic loading. Mater Struct 39 (6):621-634. doi:10.1617/s11527-005-9054-z

Harajli MH (2008) Seismic behavior of RC columns with bond-critical regions: Criteria for bond strengthening using external FRP jackets. J Compos Constr 12 (1):69-79. doi:10.1061/(Asce)1090-0268(2008)12:1(69)

Harajli MH (2009) Bond strengthening of lap spliced reinforcement using external FRP jackets: An effective technique for seismic retrofit of rectangular or circular RC columns. Cons Build Mater 23 (3):1265-1278. doi:DOI 10.1016/j.conbuildmat.2008.07.028

Helal Y (2012) Seismic strengthening of deficient RC elements using PTMS. Ph.D. thesis, Dept. of Civil and Structural Engineering, The University of Sheffield, UK, available on line: http://etheses.whiterose.ac.uk/7286/.

Karayannis CG, Chalioris CE, Sirkelis GM (2008) Local retrofit of exterior RC beam-column joints using thin RC jackets - An experimental study. Earthq Eng Struct D 37 (5):727-746. doi:Doi 10.1002/Eqe.783

Lynn AC, Moehle JP, Mahin SA, Holmes WT (1996) Seismic evaluation of existing reinforced concrete building columns. Earthq Spectra 12 (4):715-739

Melek M, Wallace JW, Conte JP (2003) Experimental assessment of columns with short lap splices subjected to cyclic loads. Pacific Earthquake Engineering Research Center, College of Engineering, University of California, Berkeley

Metelli G, Cairns J, Plizzari G (2014) The influence of percentage of bars lapped on performance of splices. Materials and Structures:1-14

Moghaddam H, Samadi M, Pilakoutas K, Mohebbi S (2010) Axial compressive behavior of concrete actively confined by metal strips; part A: experimental study. Materials and Structures 43 (10):1369-1381. doi:DOI 10.1617/s11527-010-9588-6

Mulyani R (2013) Extended framework for earthquake and tsunami risk assessment: Padang city a case study. Ph.D. thesis, Dept. of Civil and Structural Engineering, The University of Sheffield, UK

Orangun CO, Jirsa JO, Breen JE (1977) Re-evaluation of test data on development length and splices. J Am Concrete I 74 (3):114-122

Priestley MJN, Seible F (1995) Design of seismic retrofit measures for concrete and masonry structures. Const Build Mater 9 (6):365-377. doi:10.1016/0950-0618(95)00049-6

Samadi M, Moghaddam H, Pilakoutas K (2012) Seismic retrofit of RC columns with inadequate lap-splice length by external post-tensioned high-strength strips. Paper presented at the In: Proc. of the 15 World Conference on Earthquake Engineering, Lisbon, Portugal

Sause R, Harries KA, Walkup SL, Pessiki S, Ricles JM (2004) Flexural behavior of concrete columns retrofitted with carbon fiber-reinforced polymer jackets. Aci Struct J 101 (5):708-716

Sozen MA, Moehle JP (1990) Development and lap-splice lengths for deformed reinforcing bars in concrete. Portland Cement Association, Skokie, IL,

Tepfers R (1988) Overlap splices for ribbed bars for free use in a concrete structure. Nordic Concrete Research, Publication No 7. Nordic Concrete Federation, Oslo, pp. 273-283

Zuo J, Darwin D (2000) Splice strength of conventional and high relative rib area bars in normal and high-strength concrete. Aci Struct J 97 (4):630-641